ENCIT 2018

ABCM Associação Brasileira de Engenharia e Ciências Mecânicas

17th Brazilian Congress of Thermal Sciences and Engineering
November 25th-28th, 2018, Águas de Lindóia, SP, Brazil

A NUMERICAL INVESTIGATION OF ANGLE OF ATTACK EFFECTS ON AIRFOIL NOISE SECONDARY TONES

Lucas Bradaschia Mascagni Frederico
lucasmascagni@gmail.com
William Roberto Wolf
wolf@fem.unicamp.br
Universidade Estadual de Campinas, UNICAMP

Abstract. *Numerical simulations of a NACA0012 airfoil under moderate Reynolds number conditions (50.000 < Re < 100.000) are carried out in order to assess the noise generation phenomena (broadband + tonal noise) including the flow structures along the boundary layer. We employ a computational fluid dynamics tool with low dispersion and dissipation characteristics, able to resolve unsteady flow features which may occur in the mentioned conditions, such as the unsteady disturbances that appear on the airfoil surface (Tollmien-Schlichting waves) and which are amplified via an acoustic feedback mechanism near the trailing edge. This mechanism makes the shear layer highly unstable close to the trailing edge and is believed to be the cause of secondary tones observed in the noise spectra. In order to examine aspects of the flow stability and its spatial characteristics, techniques such as Fourier transform, wavelet transforms and dynamic mode decomposition are applied.*

Keywords: *Airfoil trailing-edge noise, trailing-edge instability, dynamic mode decomposition*

1. INTRODUCTION

In the past years, more severe restrictions regarding noise control in the vicinity of airports and cities pushed flight companies and airspace industries to implement new procedures and technologies to reduce aircraft self noise. Civil aircraft produce up to 30 dB less noise compared to 50 years ago (Dobrzynski, 2010), (Lilley, 2001) and even lower levels are endorsed. It is true that much of this improvement is due the success of the high bypass ratio turbofan engines and revolutionary nacelle designs, however, as these technologies reach a plateau, the self-noise generated by the airframe (which includes the wings, flaps, fuselage, landing gear, etc) has been seen as the next potential lower noise barrier (Dobrzynski, 2010).

It is known that the noise generated by an airfoil in a stationary flow is due to pressure fluctuations on its surface and a dominant source arises from the flow detachment at the trailing edge (Brooks *et al.*, 1989) associated with the vortex shedding (Patterson *et al.*, 1973). At low velocities and non-turbulent flows, the scattering at the trailing edge - or vortex shedding - is composed by coherent structures and the pressure fluctuations for an observer at the acoustic field shows a clear tonal noise. As the velocity is increased an the flow becomes transitional and, subsequently, turbulent, the coherence tends to be destroyed and, then, the noise spectrum shows more of a broadband hump as the tonal is submerged (Arbey and Bataille, 1983) and (Ramirez and Wolf, 2016).

In transitional flows at moderate Reynolds numbers (50.000 < Re < 100.000), it is possible to identify aspects of both non-turbulent and turbulent flows as the vortex shedding becomes less coherent and the broadband hump increases in the noise spectrum leading to the appearance of secondary tones, as shown in figure 1. According to (Sandberg and Jones, 2010) and (Desquenes *et al.*, 2007) it is known that small perturbations arise at the suction side (Tollmien-Schlichting waves) and are transported along the surface towards the trailing edge, where they interact with the vortex shedding, emitting stronger pressure pulses that travel back to the leading edge, amplifying new perturbations and starting a new cycle. This periodic phenomenon is know as acoustic feedback and may form interesting flow features, such as an asymmetric separation bubble near the trailing edge even for a zero degree angle of attack and a highly unstable shear layer.

The explanation of this physical mechanism, though, is still cause of some disparities among the community since there are unsolved questions regarding how the loop works, where it is closed, the possible existence of a secondary loop (Desquenes *et al.*, 2007), which frequencies are amplified at the suction side and what are the aspects of these waves. Thus, the main effort in this investigation is to understand the circumstances of the occurrence of such mechanism and aspects of its activation and continuance. In order to do so, we implement post-processing techniques such as Fourier and wavelet transforms and dynamic mode decomposition in numerical simulations obtained by a high fidelity computational fluid dynamics tool which is further explained in section 2.1

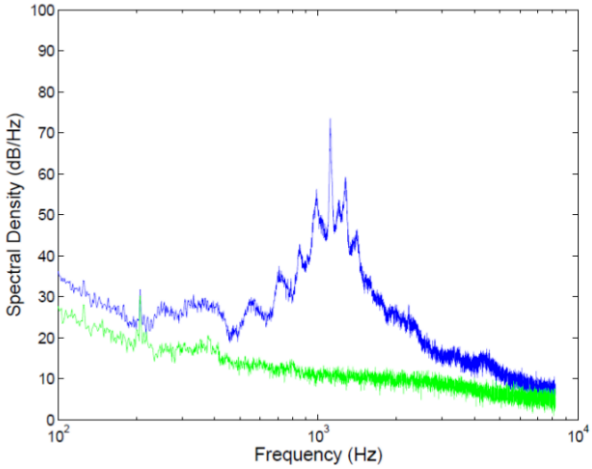

Figure 1. Experimental noise spectra for a NACA0012 under 100,000 Reynolds number flow displaying secondary tones around the main peak and a broadband hump. Blue line indicates the airfoil self-noise and green the background noise from the wind-tunnel. Extrated from (Arcondoulis *et al.*, 2009).

2. METHODOLOGY

2.1 Numerical Methods and Flow Simulations

In the present flow simulations, the general curvilinear form of the compressible Navier-Stokes equations is solved. The numerical scheme for spatial discretization is a sixth-order accurate compact scheme (Nagarajan *et al.*, 2003) implemented on a staggered grid. Compact finite-difference schemes are non-dissipative and numerical instabilities arising from mesh non-uniformities and interpolation at grid interfaces have to be filtered to preserve stability of the numerical schemes. The high wavenumber compact filter presented by Lele (1992) is applied to the computed solution at prescribed time intervals in order to control numerical instabilities. This filter is only applied in flow regions outside of boundary layers.

The time integration of the fluid equations is carried out by the fully implicit second-order scheme of Beam and Warming (Beam and Warming, 1978) in the near-wall region in order to overcome the time step restriction due to the usual near-wall fine-grid numerical stiffness. A third-order Runge-Kutta scheme is used for time advancement of the equations in flow regions far away from solid boundaries. No-slip adiabatic wall boundary conditions are applied along the solid surfaces and characteristic plus sponge boundary conditions are applied in the far field locations. The numerical tool has been previously validated for several simulations of compressible flows involving sound generation and propagation (Wolf, 2011; Wolf *et al.*, 2013). Calculations are performed using non-dimensional quantities using the freestream density, temperature and speed of sound as reference quantities, and the airfoil chord as reference length.

2.2 Methodology and Post-Processing

For practical reasons, the investigations are divided in two: (1) the emergence and amplification of first instabilities and (2) the consequent steady-state flow for positive and zero angles of attack. First, to evaluate the occurrence of the boundary layer instability phenomenon and validate the capability of the CFD tool in capturing it, we start with 2-D simulations for a number of cases in different conditions and configurations. For steady-state flows, the pressure fluctuation signal for an observer at the far-field was accessed and related to the flow features. Then, applying a discrete fourier transform (DFT) to resolve the pressure fluctuation spectrum, it was possible to check the noise radiation characteristics. The expected behavior briefly explained in the introduction is confirmed, although it was seen that mesh refinement exercises great influence on the problem, being, initially one of the major concerns.

The DFT, however, have some drawbacks, since it assumes statistical convergence of the signal, making it difficult to study the stage of amplification of the instabilities. The method also needs a great amount of samples to provide good frequency resolution, according to $\Delta f = f_s/N$, with f_s being the sampling rate and N, the number of samples. Therefore, to investigate the stability characteristics of the problem we alternate to methods such wavelet transform, which interprets a signal by stretching and translating a general wavelet form and a flow modal analysis such as dynamic mode decomposition. Furthermore, we suspect that pulses emitted from the leading edge at each cycle are composed by a wavepacket, instead of single frequencies.

2.3 Modal Analysis

Dynamic mode decomposition (DMD) is a relatively new technique introduced into the fluids mechanics community by (Schmid and Sesterhenn, 2008) and further studied by (Rowley *et al.*, 2009), (Mezic, 2013) among others. The method uses a collection of snapshots resolved in time to decompose the flow-field into spatio-temporal coherent structures - called modes - each of them associated to a single frequency of oscillation and a rate of growth/decay. The method shares a relation with the Koopman operator and according to some of these authors, the method is equivalent to the use of DFT when applied in many situations, such as a steady-state flow.

Each snapshot containing the set of variables defined by the user is arranged into column vectors x_k, where k represents the snapshot instant. So, for a number m snapshots, we construct the matrices X and X':

$$X = \begin{bmatrix} | & | & & | \\ x_1 & x_2 & \dots & x_{m-1} \\ | & | & & | \end{bmatrix} \text{ and}$$

$$X' = \begin{bmatrix} | & | & & | \\ x_2 & x_3 & \dots & x_m \\ | & | & & | \end{bmatrix}$$

The method is then based in adjusting a linear operator A that relates:

$$X' = AX$$

In other words, A is a linear operator that connects a snapshot x_k to its consecutive one. The objective of DMD is then to calculate the eigendecomposition of A in order to obtain its spatial modes and eigenvalues that characterize the system. It is possible to calculate A by simply doing $A = X'X^+$, where X^+ is the pseudo-inverse of X. However, since the number of lines in matrix X is much higher than number of columns ($m >> n$), it turns out this calculation is prohibitively inefficient. So, we applied the algorithm proposed by (Tu *et al.*, 2014).

- Singular value decomposition (SVD) of matrix X such as $X = U\Sigma V^*$ and $X^+ = U^*\Sigma^{-1}V$. Here, it is possible to truncate the SVD, considering only the first r columns of U and V, and the first r columns and rows of Σ.
- We let $\tilde{A} = U^*AU$ and make the substitutions, so $\tilde{A} = U^*X'V\Sigma^{-1}$;
- Eigendecomposition of $\tilde{A}$,
  $\tilde{A}W = W\Lambda$
  where each column of matrix W represents an eigenvector of $\tilde{A}$ and each element λ_i in diagonal matrix Λ is an eigenvalue - these already represent the DMD eigenvalues.
- To calculate the DMD spatial modes we have,
  $\Phi = X'V\Sigma^{-1}W$
  so each column of Φ is a DMD mode ϕ_i, associated to its eigenvalue λ_i .

Then, the flow variable analyzed X can be reconstructed using the following relation

$$X(x, y, t) = \sum_{i=1}^{m-1} a_i \exp(\lambda_i t)\phi_i(x, y)\,,$$

where a_i is the mode amplitude. We use it to find a set of weights to match the first point measure, so we calculate the modes amplitudes. It is interesting to mention that the acoustic feedback may also happens in full turbulent flows, although being more hard to distinguish and characterize due to the large number of spatial features and temporal scales. In that sense (when statistical convergence is unbearable), DMD may be a helpful tool.

3. RESULTS

3.1 Flow Simulations

In this section, we present results obtained by numerical simulations used to capture from the emergence of the first instabilities to the establishment of a new steady state flow pattern.

3.1.1 Angle of attack of 3 degs.

The sequence of snapshots in figure 2 shows the divergent of velocity for an airfoil at 3 deg, Mach number 0.3 and Reynolds number of 100,000, a configuration studied previously in which the acoustic feedback occurs. The first snapshot

shows the primary flow where acoustic pulses are emitted from the trailing edge at each vortex shedding. This pulses propagate with the upstream charecteristic velocity (u-c), suffering a distortion in its form due to the airfoil boundary layer. In the second snapshot, it is possible to see the first instabilities within the boundary layer that rapidly grow and are transported towards the trailing edge, as shown in the third snapshot. The fourth snapshot shows how the pressure pulses emitted tend to become more intense after the instabilities reach the trailing edge, establishing a new steady state flow pattern.

The next image (figure 3) shows a logarithmic plot of the pressure fluctuation spectrum obtained by an observer at the far-field for the steady state flow (after the instabilities have grown and became periodical). The noise spectra is obtained using 8,000 samples spaced in 0.025 time units. One can see in this figure that the far-field pressure spectrum presents the multiple tonal peaks arising from the feedback loop mechanism. A main tone is observed along with several secondary tones which are equispaced and superimposed on a broadband spectrum.

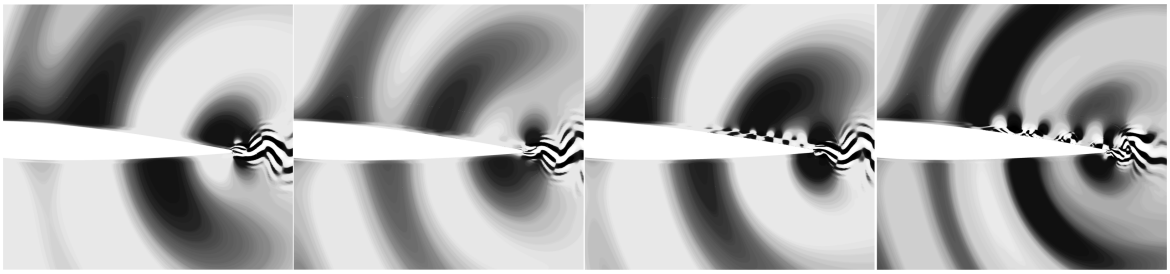

Figure 2. Sequence of snapshots for divergence of velocity displaying the emergence and continuance of instabilities for an airfoil with 3 deg angle of attack.

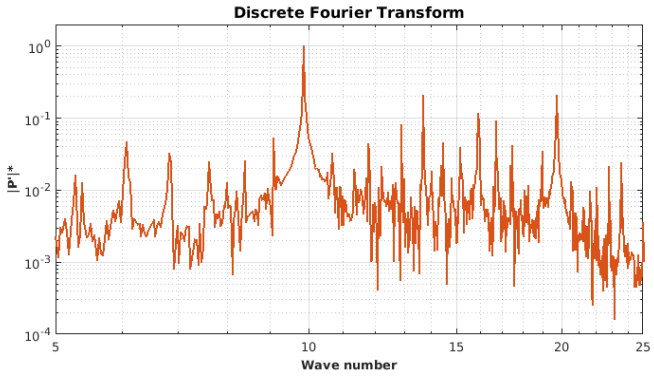

Figure 3. Pressure fluctuation spectrum for a probe at the far-field for steady state flow.

3.1.2 Angle of attack of 0 degs.

Figure 4 shows the analogue process for an airfoil at 0 deg, Mach number 0.3 and Reynolds number of 100,000. The figure displays the contour of divergence of velocity for different instants of the flow. One can see the initial flowfield and its noise generation in the first figure. Then, it is possible to observe the growth of the instabilities in the form of a wavepacket. Here, it is not so clear where the flow instabilities arise, but it is possible to check they are closer to the trailing edge. Even though this configuration is symmetric, the flow becomes non-symmetric after some time. Then, the wavepackets are visualized only along the suction or the pressure sides of the airfoil, on the vicinity of the trailing edge.

Figure 5 shows the spectrum of pressure fluctuations for an observer at the far-field for the steady-state flow (after the first perturbations are advected and a periodical regime is established). This noise spectrum is obtained using 7,000 samples spaced in 0.025 time units. The pressure spectrum is cleaner compared to that from the 3 deg. angle of attack configuration. Here, one can clearly see the multiple tonal peaks, including the main tone and the equidistant secondary tones along the broandband spectrum.

3.2 DMD Analysis

In this section, modal analysis is first applied to the steady-state flows to evaluate the methodology. The flow variable accessed is the flow pressure so we can compare the results with their respective noise spectra obtained previously. For both cases, we used a dataset composed of 800 snapshots spaced in 0.025 time units. We also truncate the singular value decomposition to consider only 100 columns and rows.

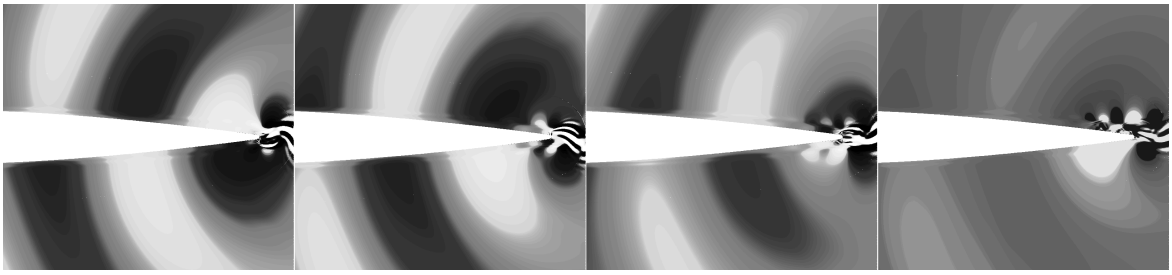

Figure 4. Sequence of snapshots for divergence of velocity displaying the emergence and continuance of instabilities for an airfoil at 0 deg.

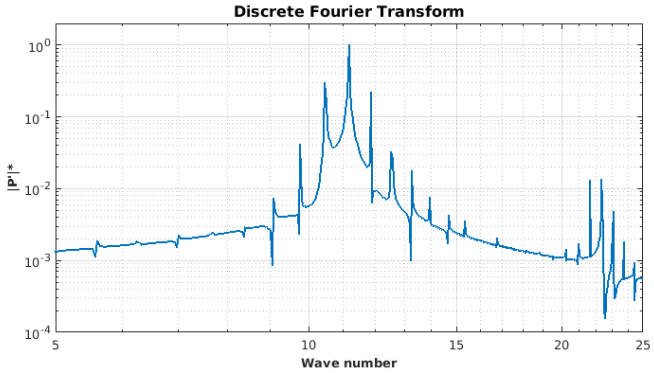

Figure 5. Pressure fluctuation spectrum for a probe at the far-field for steady-state flow.

3.2.1 Angle of attack of 3 degs.

For the positive angle of attack case, DMD provides a very good agreement with DFT indicating that the pressure modes with higher normalized amplitudes occur at the same main frequencies indicated by Fourier analysis, which was calculated for a signal captured by a probe at the far-field. The method is very efficient in disposing of the numerical errors and highlighting even the shortest peaks indicated by DFT. As expected for a steady-state case, the growth rates are all zeros or negative indicating either periodic non-damped and damped structures.

In figure 6 we display the spatial modes for the main tonal peak (mode 19) and a secondary tone (mode 27) that appear due to the acoustic feedback mechanism. The modes shown in figure 7 indicate a clear feedback relation between the pressure pulses emitted from the trailing edge with the instabilities that happen along the pressure side of the airfoil since they oscillate at the same frequencies. These instabilities seem to have a wavepacket structure.

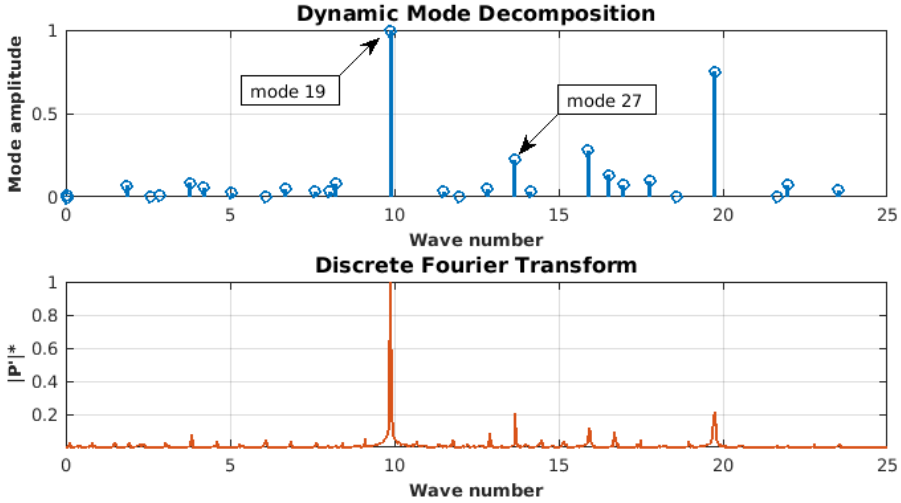

Figure 6. Normalized amplitudes for DMD and DFT indicating similar frequencies.

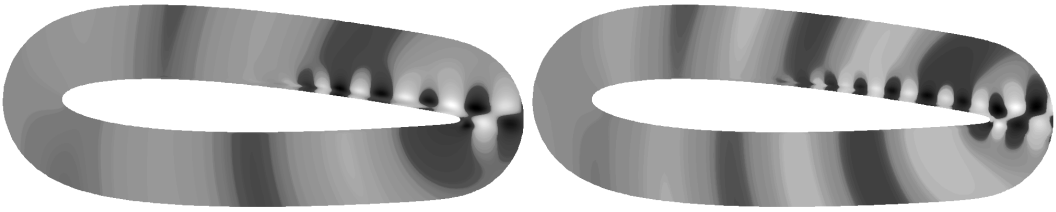

Figure 7. Spatial DMD modes for mode 19 and 27, respectively.

3.2.2 Angle of attack of 0 deg.

For the 0 deg. angle of attack case, DMD provides an even better agreement with the DFT calculated for a signal captured by a probe at the far-field, as shown in figure 8. The growth rates are also all zeros or negative, as expected. Figure 9 displays the spatial modes for the main tonal peak (mode 17) and a secondary tone (mode 14), close to it. In this case, the instabilities occur closer to the trailing edge and it is not possible to clearly identify the wavepacket structures that lead to the flow instabilities on the suction side of the airfoil, as the previous case. However, it is possible to check that these modes have very similar spatial characteristics, but different intensities, since they occur at very close frequencies.

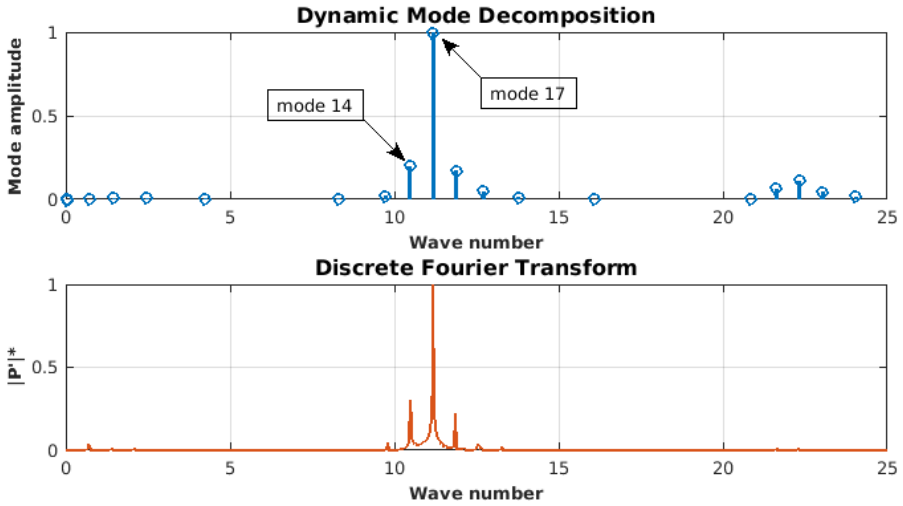

Figure 8. Normalized amplitudes for DMD and DFT indicating similar frequencies.

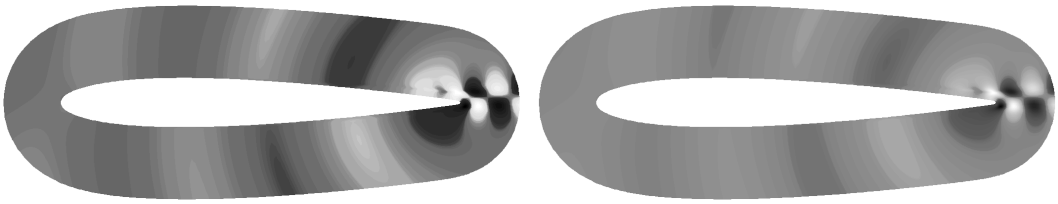

Figure 9. Spatial DMD modes for mode 17 and 14, respectively.

4. CONCLUSIONS

This work presents a study of trailing edge noise for airfoils at moderate Reynolds numbers. For both zero and 3 deg. angle of attack cases analyzed, simulations are able to verify the existence of perturbations responsible for activating an acoustic feedback phenomenon. When the angle of attack is equal to zero, it is yet unclear where the flow instabilities initiate, although it is suspected that they appear at the shear layer, close to the trailing edge. When the airfoil is at incidence, wavepacket structures are observed along the suction side of the airfoil. These structures grow initially due to the acoustic waves which propagate upstream the boundary layer. Then, they are excited by the feedback mechanism which leads to a periodic flow. In both cases investigated, it is possible to verify that secondary tones in the noise spectra are related to flows where the airfoil wake is periodically disturbed.

Modal analysis is employed together with Fourier analysis and they are able to indicate the main oscillation frequencies for the steady flow. As expected, both techniques should return similar results for the steady state flow, however, dynamic

mode decomposition has the advantage of using a much smaller database to provide similar results to DFT. The spatial modes are well resolved, indicating that the instabilities on the suction side oscillate at the same frequency of the pressure pulses from the trailing edge. As expected for stationary flows, all modes are stable or have negative decay rates. The modes associated to secondary tones close to the main tone mode show little discrepancies to the latter. We will present a DMD analysis for the transient portion of the current flows in the final paper and further investigations of the flow stabilities.

5. ACKNOWLEDGEMENTS

The work is partially supported by Fundação de Amparo à Pesquisa do Estado de São Paulo, FAPESP, under Research Grants No. 2013/07375-0 and No. 2013/03413-4. The support provided by FUNCAMP, project 5201, through a scholarship for the first author is likewise gratefully appreciated. The computational resources provided by CENAPAD-SP under Project No. 551 are also acknowledged.

6. REFERENCES

Arbey, H. and Bataille, J., 1983. "Noise generated by airfoil profiles placed in a uniform laminar flow". *Journal of Fluid Mechanics*, Vol. 134.

Arcondoulis, E.J.G., Doolan, C.J. and Zander, A.C., 2009. "Airfoil noise measurements at various angles of attack and low reynolds number". *ACOUSTICS 2009*.

Beam, R.M. and Warming, R.F., 1978. "An implicit factored scheme for the compressible Navier-Stokes equations". *AIAA Journal*, Vol. 16, pp. 393–402.

Brooks, T.F., Pope, D.S. and Marcolini, M.A., 1989. "Airfoil self-noise and prediction". *NASA Reference Publication*, Vol. Technical Report 1218.

Desquenes, G., Terracol, M. and Sagaut, P., 2007. "Numerical investigation of the tone noise mechanism over laminar airfoils". *Journal of Fluid Mechanics*, Vol. 591.

Dobrzynski, W., 2010. "Almost 40 years of airframe noise research: what did we achieve?" *Journal of Aircraft*, Vol. 47, pp. 353–367.

Lele, S.J., 1992. "Compact finite difference schemes with spectral-like resolution". *Journal of Computational Physics*, Vol. 103, pp. 16–42.

Lilley, G.M., 2001. "The prediction of airframe noise and comparison with experiment". *Journal of Sound and Vibration*, Vol. 239, pp. 849–859.

Mezic, I., 2013. "Analysis of fluid flows via spectral properties of the koopman operator". *Annu. Rev. Fluid Mech.*, Vol. 45.

Nagarajan, S., Lele, S.K. and Ferziger, J.H., 2003. "A robust high-order compact method for large eddy simulation". *Journal of Computational Physics*, Vol. 191, No. 2, pp. 392–419.

Patterson, R., Vogt, P., Fink, M. and Munch, G., 1973. "Vortex noise of isolated airfoils". *Society of Naval Architects and Marine Engineers, and U.S. Navy, Advanced Marine Vehicles Meeting*.

Ramirez, W.A. and Wolf, W.R., 2016. "Effects of trailing edge bluntness on airfoil tonal noise at low reynolds numbers". *J. Braz. Soc. Mech. Sci. Eng*, p. 2369âĂŞ2380.

Rowley, C.W., MeziÄĞ, I., Bagheri, S., Schlatter, P. and Henningson, D.S., 2009. "Spectral analysis of nonlinear flows". *Journal of Fluid Mechanics*, Vol. 641.

Sandberg, R. and Jones, L., 2010. "Direct numerical simulations of airfoil self-noise". *Procedia Engineering*, Vol. 6.

Schmid, P.J. and Sesterhenn, J., 2008. "Dynamic mode decomposition of numerical and experimental data". *Journal of Fluid Mechanics*, Vol. 656.

Tu, J.H., Rowley, C.W., Luchtenburg, D.M., Brunton, S.L. and Kutz, J.N., 2014. "On dynamic mode decomposition: theory and applications". *J. Comput. Dyn.*, Vol. 1.

Wolf, W.R., 2011. *Airfoil aeroacoustics, LES and acoustic analogy predictions*. Ph.D. thesis, Stanford University, Stanford.

Wolf, W.R., Azevedo, J.L.F. and Lele, S.K., 2013. "Effects of mean flow convection, quadrupole sources and vortex shedding on airfoil overall sound pressure level". *Journal of Sound and Vibration*, Vol. 332, pp. 6905–6912.

7. RESPONSIBILITY NOTICE

The following text, properly adapted to the number of authors, must be included in the last section of the paper:
The author(s) is (are) the only responsible for the printed material included in this paper.